Available online at www.sciencedirect.com

ScienceDirect

Procedia Manufacturing 26 (2018) 198–204

Procedia MANUFACTURING

www.elsevier.com/locate/procedia

46th SME North American Manufacturing Research Conference, NAMRC 46, Texas, USA

Microstructural and Metallurgical Assessment of the Laser-Patterned Cemented Tungsten Carbide (WC-CoNi)

Shiqi Fang[a,b], Flavio Soldera[c], Andreas Rosenkranz[c], Thomas Herrmann[d], Dirk Bähre[a,*], Luis Llanes[b], Frank Mücklich[c]

[a]*Institute of Production Engineering, Saarland University, Saarbrücken, 66123 Germany*
[b]*CIEFMA – Dept. Materials Science and Metallurgical Engineering, Universitat Politècnica de Catalunya, Barcelona, 08028, Spain*
[c]*Chair of Functional Materials, Saarland University, Saarbrücken, 66123, Germany*
[d]*Photonik-Zentrum Kaiserslautern e.V., 67663 Kaiserslautern, Germany*

* Corresponding author. Tel.: +49 (0)681 302 3075; fax: +49 (0)681 302 4858.
E-mail address: d.baehre@mx.uni-saarland.de

Abstract

Cemented carbide is difficult to machine using traditional chip-removal methods due to its hardness. Electrical discharge machining (EDM) is the common method applied to shape cemented carbides because high geometric precision can be achieved. However, some important defects (pores, residual stresses or oxidation products) can be induced due to thermal reactions. Ultra-short pulse laser processing can also provide high precision and meanwhile effectively avoid these defects due to its short laser-matter reaction time. In this paper, three different patterns on WC-CoNi cemented carbides for tribological purposes, namely line-like patterns, dimples and grooves, have been created using different laser set-ups with pulse duration in the range of nanoseconds (10^{-9}s), picoseconds (10^{-12}s) and femtoseconds (10^{-15}s). Microstructural and metallurgical changes of modified surfaces have been studied. Laser scanning microscopy (LSM) is conducted to measure the pattern dimensions. Focused ion beam (FIB) in combination with scanning electron microscope (SEM) is used to investigate the microstructural changes of the patterned materials.

Peer-review under responsibility of the scientific committee of the 46th SME North American Manufacturing Research Conference.

Keywords: Cemented carbide; Ultra-short pulse laser processing; Laser surface patterning (LST); Surface integrity

1. Introduction

Cemented tungsten carbide, often referred to as hardmetal, is produced by sintering tungsten carbide (WC) with cobalt (Co) or Nickel (Ni) powder under high pressure and temperature. Cemented carbide is often used as cutting tool material due to its adequate hardness in combination with toughness and high thermal resistance. It is reported that WC has a melting point of about 2720 °C and density of 15.7g/cm³ [1].

Cemented Carbide is harder than most steels, and its hardness can reach 1600HV30 [2]. EDM is one of the most advanced hardmetal processing technologies applied in the industry whereby high geometric precision can be achieved based upon the non-contact thermal machining processes [3,4]. Research work presented in [5,6] indicates that the material is removed by the thermal reactions resulting from numerous tiny sparking erosions between the electrodes. Additionally, the mechanical properties of the machined surfaces can be strongly influenced in the processes. Meanwhile, some unexpected defects, such as micro-cracks, oxidation, re-deposition and pores can be induced in the heat affected zones.

Since the early 1990s, ultra-short pulse (10^{-12}s-10^{-15}s) laser processing has been used as a surface treatment in order to improve the tribological performance of functional surfaces due to its high accuracy and excellent surface quality [7,8]. The surface treatment technique by ultra-short pulse laser processing can be named as laser surface texturing (LST). Current research validates the view that LST is a clean, fast and precise surface treatment technique. It is well accepted that LST is suitable to produce diverse patterns for engineering applications, especially for tooling [9,10]. In previous research on hardmetals, there is also confirmatory evidence that hardmetals are machinable by ultra-short pulse laser processing. Further evidence indicates that new patterns (dimples, grooves, etc.) can reduce the contact area as well as diminish the coefficient of friction (COF) in the tribological system, e.g., the cutting surfaces [11-13]. However, there is not enough research work available dealing with the surface integrity of hardmetal surfaces for tribological purposes modified by LST. Therefore, it is deemed to investigate the hardmetal surface integrity in terms of microstructural and metallurgical modification.

2. State of the art

The quality of surface patterns produced by laser processing can be influenced by many factors, for instance, laser beam quality and absorption characteristics (surface conditions and targeted materials). Regarding the laser parameters, energy density, wavelength and pulse duration are the most important intrinsic impact factors.

Energy absorption rate as well as spot size is ... wavelength is 1064 nm, and the absorption increase is limited when the wavelength decreases [11, 14]. Given that WC and Co have the respective melting and vaporisation temperatures (WC: 3143 K, 6273 K; Co: 1768 K, 3170 K) [15], it is obvious that Co will be firstly melted and ablated due to the large melting temperature gap between the two components. Within this context, the energy density (fluence) leads to different material removal sequences: Co can be selectively ablated at the fluence between 0.6 and 2.5 J/cm² in the nanosecond regime. However, when the fluence is less than 0.6J /cm², no evident vaporization is observed [13, 16].

Pulse duration is the decisive parameter with regard to laser-matter interaction mechanism. It can be observed that two different material removal mechanisms occur when the pulse duration overpasses ~1 ps [17]. In the femtosecond regime, the material is removed mainly by the cold ablation as a consequence of coulomb explosion. This can be explained by the fact that there is not enough time to establish electron-photon coupling and to transfer the energy to the lattice. In the nanosecond regime, the material is removed by phase transformations (melting and vaporisation) resulting from the local temperature rising induced by the laser. In the picosecond regime, a mixture of the aforementioned processes typically occurs.

The term surface integrity is used to describe the surface and subsurface conditions of a machined area [18,19]. In this work, the characterization especially focuses on two aspects: microstructural changes within the surface layer and identifying the introduced surface damages.

3. Materials & experimental procedure

3.1. Materials

The studied hardmetal possesses 14% cobalt and in addition to this 14% nickel in weight. The WC grains have an average size of 20 µm (Table 1). Three specimens with a dimension of 20 ×3 ×5 mm³ have been produced by EDM. Fig 1(a,b) presents the surface and microstructural characterization of the sample subsurface after the EDM processing. The Focus Ion Beam (FIB) was used to assess the microstructural changes. It is obvious that the thermal reactions have important influence on the surface.

[20,21]. Therefore, the surface should be fine polished before the laser treatment. Subsequently, three representative patterns, namely line-like patterns, dimples and grooves, were produced on the polished surfaces using nano-, pico- and femto-second laser, respectively.

Table 1. Microstructural characteristics and properties of the used WC-CoNi hardmetal.

WC Grain Size (μm)	Co (wt%)	Ni (wt%)	Density (g/cm^3)	Hardness (HV30)
Coarse	14	14	12.82	610

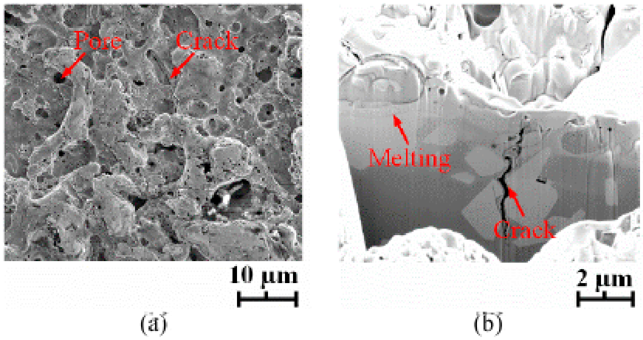

Fig. 1. (a) Surface and (b) microstructural characterization of the cemented carbide surface after EDM processing.

3.2. Experimental parameters

Table 2 summarizes the experimental parameters of the respective laser set-ups. The line-like patterns have been produced using a nanosecond Nd: YAG laser (Spectra Physics Quanta Ray Pro 290). The laser beams have a pulse repetition frequency (PRF) of 10 Hz, wavelength of 355 nm, pulse duration of 10 ns. The fluence was kept constant at around 2.3 J/cm^2. Special configurations of the laser beam trajectories are necessary to obtain the line-like pattern with defined geometry [22,23]. Fig. 2(a) shows the trajectory of the respective laser beams: the primary beam goes through a lens and is then split into two equal sub-beams by a beam splitter. The sub-beams are reflected by mirrors and finally interfere on the target surface. The dimples have been created using a picosecond laser system (Fig. 2(b), HYPER25 Coherent Kaiserslautern GmbH,). The used PRF is 200 kHz and the wavelength is set to 532 nm. The fluence was kept constant at 0.5J/cm^2. The grooves have been produced using a passively mode-locked ultra-short pulse Ti:Sapphire laser (Fig. 2(c), Spitfire, wavelength 800 nm and pulse duration (FWHM) 150 ± 7 fs, respectively. The fluence was set to 0.05 J/cm^2. The laser beam moves at the speed of 1 mm/s.

Table 2. Experimental parameters of the laser set-ups.

Laser type	Laser source	Pulse duration	Wave length (nm)	PRF (Hz)	Fluence (J/cm^2)
ns-laser	Nd: YAG	10 ns	355	10	2.3
ps-laser	HYPER25	10 ps	532	200 K	0.5
fs-laser	Ti:Sapphire	150 fs	800	1000	0.05

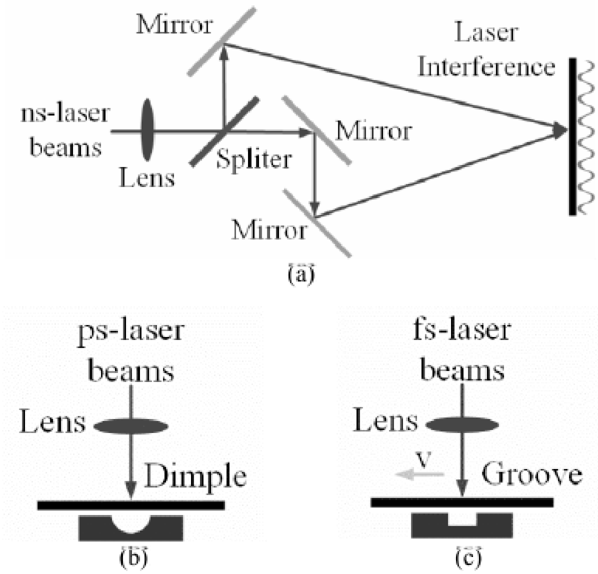

Fig. 2. Schematic illustrations of experimental laser set-ups: (a) ns-laser interference, (b) ps-laser, (c) fs-laser.

4. Results and discussion

4.1. Geometric characterization

Fig.3 shows the geometric properties of the produced patterns measured by LSM. For each specific pattern, measurements at five different positions were carried out to obtain their geometrical features. Average mean values of the geometrical parameters are then obtained accordingly. It is found that he line-like pattern (Fig. 3(a) and (b)) has the periodicity of 11.8 μm and the height of 0.6 μm, the dimples (Fig. 3(c) and (d)) have the diameter of 51.3 μm and the depth of 3.8 μmm, and the grooves (Fig. 3(e) and (f)) have the width of 100 μm and the depth of 1.8 μm. The deviations of the measured geometrical

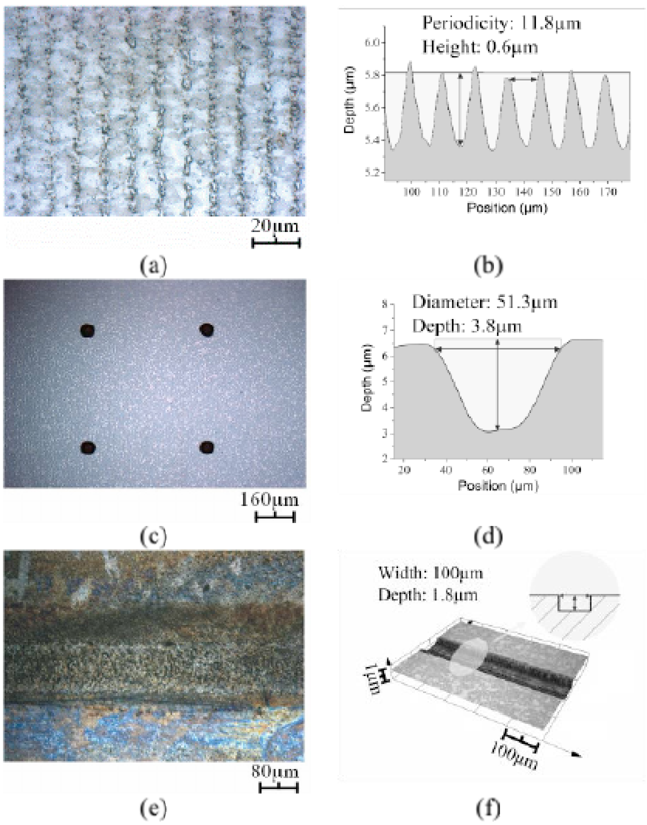

Fig. 3. LSM images and cross-sectional plots of geometric properties of surface patterns: (a) and (b) line-like pattern, (c) and (d) dimples, (e) and (f) groove.

4.2. Microstructural and metallurgical changes

- Line-like patterns

Fig. 4 shows the microstructural investigation of line-like patterns (produced by the two-beam interference using a nanosecond laser). The superposition of the two laser beams leads to a periodical energy input with laser intensity minima and maxima positions. At the position of a laser intensity maximum, the underlying material is melted. Due to surface temperature and tension gradient, the material is shifted from the hot to the cold regions (laser intensity minimum). In Fig. 4(a), the line-like pattern is not continuous, but rather interrupted. The cross-section shows that the patterns have a wavy profile (Fig. 4(b)). An enlarged view of the cross-section at a topographic maximum position (Fig. 4(c)) reveals that the lack of binder produces discontinuities. The remaining WC recrystallizes and produces the maximum. This behavior can be traced temperatures [15]. Therefore, the binder is melted and vaporized whereas the WC grains are just slightly melted but not vaporized, since the used fluence 2.3 J/cm² is not sufficient to vaporize both components [13,16]. Cracks as well as some pores, which are formed by the binder vaporization and thermal residual stress, can be observed in Fig. 4(d).

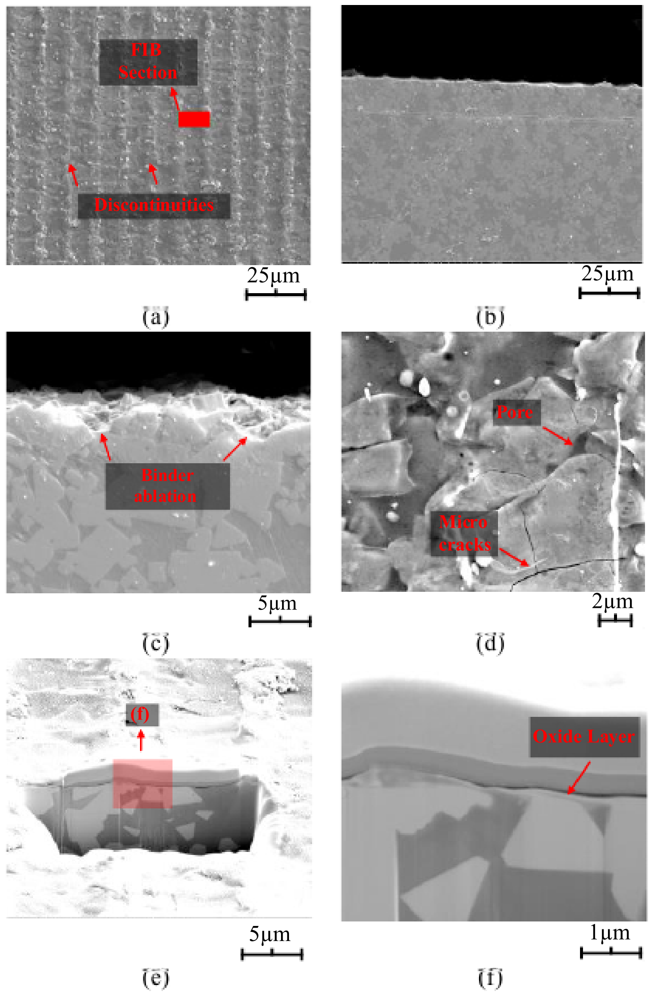

Fig. 4. Microstructural investigation of the line-like surface pattern: (a) overview, (b) cross-section, (c) enlarged view of the cross-section, (d) induced defects, (e) FIB cross-section, (e) enlarged view of the FIB cross-section.

A local cross-section ($15\times10\times6$ µm³) was done by FIB in order to study the microstructural evolution after laser processing. Fig. 4 (e) provides an overview of the cross-section whereas in the enlarged views (Fig. 4(e) and (f)) no evident thermal defects can be found. Only a very thin film (less than 0.2 µm) is visible at the surface, which differs from the initial surface morphology. It might be the oxide layer induced by the thermal diffusion [11, 24]. The oxide layer appears at the topographic minimum position of the line-like pattern, which suggests heat diffusion is more evident at the laser intensity maximum position.

- Dimples

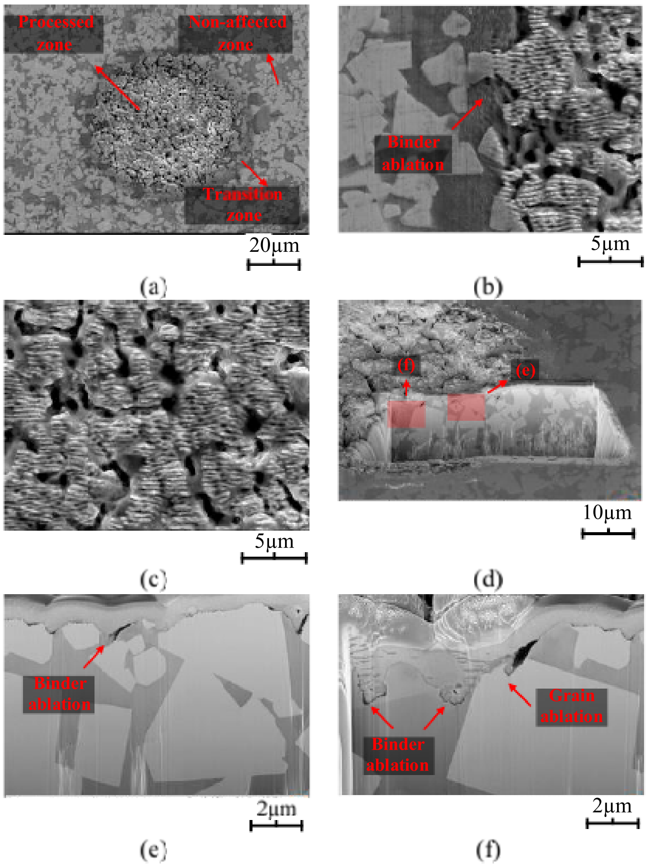

Fig. 5. Microstructural investigation of the dimples: (a) overview, (b) transition zone, (c) enlarged view of the processed zone, (d) FIB cross-section, (e) enlarged view in the transition zone, (f) enlarged view in the processed zone.

The dimples are produced by picosecond laser processing. Three zones can be observed (Fig. 5(a)): non-affected, transition and processed zones. The non-affected zone is situated outside of the laser spot. The transition zone, situated between the non-affected zone and the processed zone (Fig. 5(b)), is about 3-5 µm wide. The binder is found to be slightly melted and more affected than WC grains. This behaviour can be produced by heat diffusion [11, 15]. In the processed zone (Fig. 5(c)), the binder is gradually removed from the outer to the inner side, and ripples can be observed on the WC grains as well as on the binder. In the centre of the dimples, the binder is completely removed. It is remarkable that the remaining WC grains form a skeleton structure, because only the binder has been vaporized. Thus, some pores can be found between adjacent WC grains.

The FIB cross-section reveals the microstructure under the processed surface. The section has a dimension of $60 \times 15 \times 10\ \mu m^3$(Fig. 5(d)), covering the aforementioned three zones. In the transition zone (Fig. 5(e)), the sectional analysis shows that WC-grains have less ablation than the binder under this machining condition. The binder between WC grains is gradually ablated by the laser beams. In the processed zone (Fig. 5(f)), both binder and WC grains have been ablated and more evidently than in the transition zone. The binder ablation is about 2µm in the processed zone, and less than 1µm in the transition zone. Thus the surface appears a relatively rough topography and a skeleton structure is formed.

- Grooves

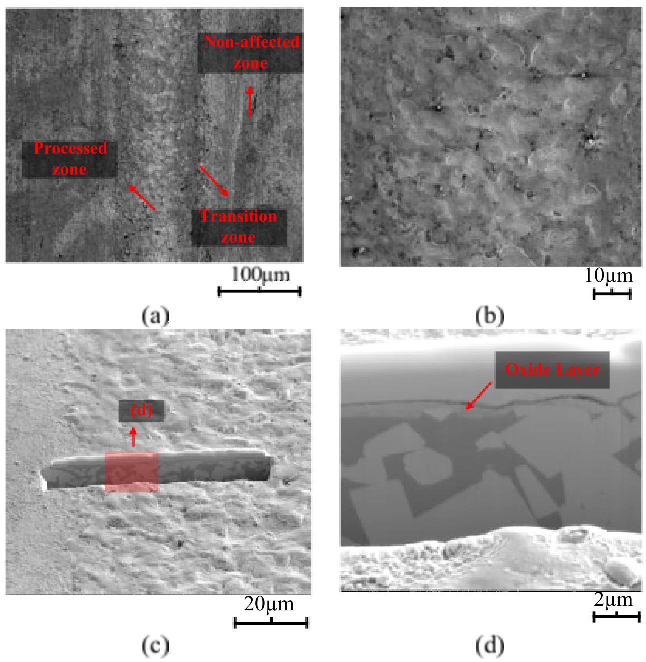

Fig. 6. Microstructural investigation of the grooves: (a) overview, (b) enlarged view of the processed zone, (c) FIB cross-section, (d) enlarged view of the FIB cross-section.

The grooves have been machined by the femtosecond laser processing. Three zones can be identified from the overview (Fig. 6(a)). The processed zone is situated in the centre and has the width of 100 µm. The affected zones can be found at both sides of the processed zone having a width of 25 µm. In Fig. 6(b), it can be seen that the processed zone appears to be blurred and to be covered by a dark layer.

zone, which has a dimension of 50×10×6 μm^3. It has been found that the oxide layer covering the processed zone has the thickness of 1 μm as shown in Fig. 6(d). No obvious defects have been detected under the oxide layer.

5. Conclusion and remarks

The microstructural changes and metallurgical conditions of the three patterns produced on a cemented carbide grade using different laser sources have been investigated. In general, the damage on the surface, having a strong impact on the geometrical accuracy, occurred mainly in the form of irregular ablation of the two different components. The stack of the redeposition usually leads to the irregularity of the structure shape. Other common defects, such as cracks, did not penetrate into the subsurface. In the case of nanosecond laser, a thin layer of oxide was produced. However, all these scenarios are observed at the very shallow position in the sub-surface, i.e. with a depth of less than 2μm. Compared to the non-laser based texturing method for hardmetals, such as EDM, less surface damage can be achieved using LST, and accordingly better geometrical accuracy can then be achieved. These major findings state that surface patterns can be fabricated with a high geometric precision and minor thermal defects.

- Line-like patterns having a periodicity of 11.8 μm and height of 0.6 μm produced by nanosecond laser processing using a fluence of 2.3 J/cm² are arranged on the surface in the square form. The molten binder forms the periodical profile resulting from the interference of two laser beams. The pattern discontinuity can be explained by the fact that the binder is vaporized more easily due to its lower melting and vaporization temperatures compared with WC grains. Some detected cracks suggest that thermal defects are still present being typical in the nanosecond regime.
- Dimples with a diameter of 51.8 μm and depth of 3.8 μm have been produced using picosecond laser processing at a fluence of 0.5 J/cm². Three zones can be identified: non-affected, transition and processed zones. The transition zone has a width of roughly 5 μm where the binder melts initially. In the affected zone, research on the morphology demonstrates that the binder has been ablated significantly and a skeleton structure is formed. much higher ablation than WC grains. There is no evidence about the re-deposition of molten material on the surfaces. It has been proved that LST under these conditions is suitable to selectively machine cemented carbides.
- Grooves with a width of 100 μm and depth of 1.8 μm have been fabricated by femtosecond laser processing using a fluence of 0.05 J/cm². It is remarkable that an oxide layer is formed and covered the processed surface. The layer has a thickness around 1 μm and no evident damages have been found under the layer.

LST of hardmetal is sensitive to the fluence, which influences significantly the material removal mechanism. At a fluence of 2.3 J/cm², both WC and binder can be melted, but only binder is vaporized. At a fluence of 0.5 J/cm², solely binder can be melted and vaporized. Finally, at a fluence of 0.05 J/cm², nothing but binder can be melted. Therefore, it can be concluded that it is absolutely necessary to select an appropriate fluence. The utilization of an adequate fluence allows for only the removal of the binder to maximum extend. The laser pulse duration impacts the laser-matter interaction: in the picosecond and femtosecond regime, the thermal defects can be efficiently avoided compared with in the nanosecond regime.

Acknowledgements

The work leading to this publication was supported by the German Academic Exchange Service (DAAD) with funds from the German Federal Ministry of Education and Research (BMBF) and the People Program (Marie Curie Actions) of the European Union's Seventh Framework Program (FP7/2007-2013) under REA grant agreement n° 605728 (P.R.I.M.E. – Postdoctoral Researchers International Mobility Experience). Finally, this contribution has also been partly funded by the Spanish Ministry of Economy and Competitiveness through Grant MAT2015-70780-C4-3P (MINECO/FEDER). The authors are grateful for the material supplier Saar-Hartmetall und Werkzeuge GmbH.

References

[1] Wolfe TA, Jewett TJ, Singh Gaur RP. Comprehensive Hard Materials. Comprehensive Hard Materials, Elsevier; 2014, p.

[2] Cardarelli F. Materials Handbook — a concise desktop reference. Materials & Design 2008;22:237. doi:10.1016/S0261-3069(00)00075-3.
[3] Casas B, Wiklund U, Hogmark S, Llanes L. Adhesion and abrasive wear resistance of TiN deposited on electrical discharge machined WC-Co cemented carbides. Wear 2008;265:490–6. doi:10.1016/j.wear.2007.11.016.
[4] Koshy P, Tovey J, Performance of electrical discharge textured cutting tools, CIRP Annals, 2011;60/1:153–156, DOI:10.1016/J.CIRP.2011.03.104.
[5] Gadalla AM, Tsai W. Electrical Discharge Machining of Tungsten Carbide-Cobalt Composites. Journal of the American Ceramic Society 1989;72:1396–401. doi:10.1111/j.1151-2916.1989.tb07660.x.
[6] Pandit SM, Rajurkar KP, Shaw MC. Analysis of Electro Discharge Machining of Cemented Carbides. CIRP Annals - Manufacturing Technology. 1981;30(1):111–6.
[7] Kawasegi N, Sugimori H, Morimoto H, Morita N, Hori I, Development of cutting tools with microscale and nanoscale textures to improve frictional behavior, Precision Engineering, 2009;33/3:248–254, DOI:10.1016/j.precisioneng.2008.07.005.
[8] Deng J, Lian Y, Wu Z, Xing Y, Performance of femtosecond laser-textured cutting tools deposited with WS2 solid lubricant coatings, Surface and Coatings Technology, 2013;222:135–143, DOI:10.1016/j.surfcoat.2013.02.015.
[9] Enomoto T, Sugihara T, Improving anti-adhesive properties of cutting tool surfaces by nano-/micro-textures, CIRP Annals - Manufacturing Technology, 2010;59/1:597–600, DOI:10.1016/j.cirp.2010.03.130.
[10] Sugihara T, Enomoto T, Crater and flank wear resistance of cutting tools having micro textured surfaces, Precision Engineering, 2013;37/4:888–896, DOI:10.1016/J.PRECISIONENG.2013.05.007.
[11] Dumitru G, Lüscher B, Krack M, Bruneau S, Hermann J, Gerbig Y. Laser processing of hardmetals: Physical basics and applications. International Journal of Refractory Metals and Hard Materials 2005;23:278–86. doi:10.1016/j.ijrmhm.2005.04.020.
[12] Obikawa T, Kamio A, Takaoka H, Osada A, Micro-texture at the coated tool face for high performance cutting, International Journal of Machine Tools and Manufacture, 2011;51/12:966–972, DOI:10.1016/J.IJMACHTOOLS.2011.08.013.
[13] Li T, Lou Q, Dong J, Wei Y, Liu J. Modified surface morphology in surface ablation of cobalt-cemented tungsten carbide with pulsed UV laser radiation. Applied Surface Science 2001;172:331–44. doi:DOI: 10.1016/S0169-4332(00)00881-3.
[14] Wang XC, Laoui T, Bonse J, Kruth JP, Lauwers B, Froyen L. Direct selective laser sintering of hard metal powders: Experimental study and simulation. International Journal of Advanced Manufacturing Technology 2002;19:351–7. doi:10.1007/s001700200024.
[15] Dieter W. Bäuerle. Laser Processing and Chemistry. Springer, vol. 208, 2011, p. 760–767. doi:10.1524/zpch.1999.208.Part_1_2.291a.
[16] Li T, Lou Q, Dong J, Wei Y, Liu J. Phase transformation during surface ablation of cobalt-cemented tungsten carbide with pulsed UV laser. Applied Physics A 2001;73:391–7. doi:10.1007/s003390100745.
ablation of solids. Applied Physics A: Materials Science & Processing 1996;63:109–15. doi:10.1007/s003390050359.
[18] M'Saoubi R, Outeiro JC, Chandrasekaran H, Jr. OWD, Jawahir IS. A review of surface integrity in machining and its impact on functional performance and life of machined products. International Journal of Sustainable Manufacturing 2008;1:203–36. doi:10.1504/IJSM.2008.019234.
[19] Field M., Kahles J.F. The Surface Integrity of Machined and Ground High Strength Steels, DMIC Report 1964; 210: 54-77.
[20] Llanes L, Mart E, Ida E, Casas B, Esteve J. Infuence of electrical discharge machining on the sliding contact response of cemented carbides. International Journal of Refractory Metals and Hard Materials 2001;19:35–40.
[21] Llanes L, Casas B, Idanez E, Marsal M, Anglada M. Surface integrity effects on the fracture resistance of electrical-discharge-machined WC-Co cemented carbides. Journal of the American Ceramic Society 2004;87:1687–93.
[22] Mücklich F, Lasagni a., Daniel C. Laser interference metallurgy - Periodic surface patterning and formation of intermetallics. Intermetallics 2005;13:437–42. doi:10.1016/j.intermet.2004.07.005.
[23] Duarte M, Lasagni A, Giovanelli R, Narciso J, Louis E, Mücklich F. Increasing lubricant film lifetime by grooving periodical patterns using laser interference metallurgy. Advanced Engineering Materials 2008;10:554–8. doi:10.1002/adem.200700321.
[24] D'Alessandria M, Mücklich F. Tailoring the chemical behavior of aluminum for selective etching by laser interference metallurgy. Applied Physics A 2009;98:311–20. doi:10.1007/s00339-009-5398-5.